Single Molecules in an Extension Clamp: Extracting Rates and Activation Barriers

Yohichi Suzuki and Olga K. Dudko

Phys. Rev. Lett. **110**, 158105 — Published 12 April 2013

DOI: 10.1103/PhysRevLett.110.158105

Single Molecules in an Extension Clamp: Extracting Rates and Activation Barriers

Yohichi Suzuki and Olga K. Dudko
Department of Physics and Center for Theoretical Biological Physics, University of California at San Diego, La Jolla, CA 92093
(Dated: March 22, 2013)

When a macromolecule, held at a fixed end-to-end separation, undergoes conformational rearrangements, the fluctuating mechanical force generated by the molecule can be used as a reporter of the molecular conformational dynamics. We present an analytical framework for extracting the intrinsic rates of conformational transitions and the locations and heights of the rate-limiting barriers from such extension clamp measurements. The unique nature of the bias imposed by the extension clamp on the activation barriers allows access to biomolecular transitions currently not accessible in pulling experiments. A mapping rule is established between the outputs of different types of experiments, providing information about poorly accessible regions of the molecular landscape.

PACS numbers: 87.15.Cc, 87.10.-e, 82.37.Rs

The remarkable capability of single-molecule techniques to apply a stretching force to individual biomolecules makes it possible to induce, trace, modify and quantify conformational rearrangements within and between biomolecules [1]. Single biomolecules are usually manipulated in a force clamp, which applies a constant force [2–4], or in a force ramp, which changes the applied force at a given rate [5, 6]. These experiments trace the molecular conformational changes through the fluctuating end-to-end extension of the molecule. But what if, instead, one "clamps" the end-to-end extension? Then, the mechanical force needed to keep the extension of the biomolecule constant could be used to trace the molecular conformational dynamics.

Instruments that clamp the extension of biological materials have long existed in the field of muscle physiology [7]. Position clamps based on laser-trap deflection [8] and on laser-light modulation [9] were developed and used successfully during the late 1990's to explore the nanomechanical properties of myosin, RNA polymerase, kinesin, and DNA [10]; this isometric regime was later investigated theoretically [11, 12]. The latest advanced extension clamp is the ultra-stable atomic force microscope [13], capable of holding the extension of a biomolecule constant over unprecedentedly long time intervals of hundreds of seconds [14]. A force sensor monitors the force produced by the molecule as it samples conformational states. In a window of values of the molecular extension X, the force "hops" between different states, revealing unfolding-refolding transitions within the biomolecule [14]. Temporal traces of the force, rich in back-and-forth transitions, yield the extension-dependent lifetimes, $\tau_{\rightarrow}(X)$ and $\tau_{\leftarrow}(X)$, of the folded and unfolded states.

This Letter provides a theoretical framework for interpreting extension clamp measurements in terms of the kinetics and energetics of macromolecules. The theory (i) treats conformational dynamics as diffusion on a free energy landscape altered by the extension clamp, (ii) accounts for the switched roles of the control parameter and observable, specific to the extension clamp, and (iii) accounts for the anharmonic nature of the unfolded state of a macromolecule. The theory is solved analytically for the key experimental outputs, the unfolding and refolding lifetimes, $\tau_{\rightarrow}(X)$ and $\tau_{\leftarrow}(X)$. The closed form of the solutions makes them readily suitable for a fit to experimental data, providing non-equilibrium and equilibrium information about the system: the intrinsic unfolding and refolding rates, the locations and heights of the activation barriers, and the equilibrium free energy. We find that the nature of the bias imposed by the extension clamp on the molecular energy landscape enhances the otherwise scarce exchange between conformations, and makes persistent the reversible transitions that only occur transiently in conventional pulling modes. We establish a mapping between measurements acquired in different manipulation modes that allows transformation into, and direct comparison between, one scheme or the other.

The extension clamp pulling scheme can be captured by a minimalist model drawn in Fig.1, where the macromolecule is represented by two components, the one undergoing conformational changes (the "molecule") and the one that remains unstructured (the "linker"). This representation is equally applicable to the experiments where the "molecule" and the "linker" are different segments of the same biomolecule, as in the case of a helical membrane protein (Fig.1A) or a polyprotein, as well as to the experiments where the linker is a foreign molecule, e.g. a DNA tethered to a protein. The molecule is attached to a stationary surface at one end and to the linker at another, fluctuating, end $x = x(t)$. The linker, in turn, is attached to a pulling device that maintains the total molecule-linker extension X constant via a feedback. Specifically, when an independent structural element of the molecule unfolds and, consequently, the molecular extension $x(t)$ increases, the pulling device is moved toward the molecule to cancel out the would-be increase in total extension X. The reverse is done for refolding. Moving the spring-like pulling device toward the molecule (upon

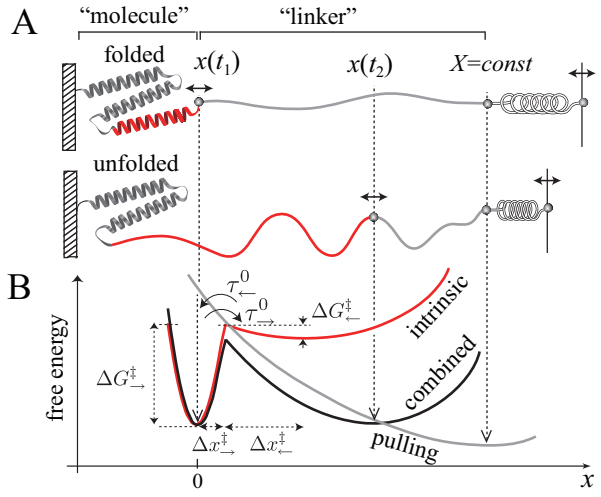

FIG. 1: Minimal model of a macromolecule in an extension clamp: the "molecule" undergoes structural changes, the "linker" remains unstructured. (a) A structural element (helix) fluctuates between the folded and unfolded conformations. As the result, the end-to-end separation $x(t)$ of the "molecule" fluctuates while the total extension X of the construct is held constant. The conformational dynamics is monitored through the force exerted by the construct on the force probe (spring). (b) The combined potential is the sum of the molecular intrinsic potential $G_0(x)$ and the "pulling" potential $G_{pull}(X-x)$. Parameters (indicated) of the intrinsic potential can be extracted from the fit of the extension clamp lifetimes to the analytical solutions in Eq.(3).

unfolding) or away from it (upon refolding), while keeping the total extension X constant, results in a change in the extension of the pulling spring and, hence, a force that "hops" between a higher value $F_{\rightarrow}(X)$ in the folded state and a lower value $F_{\leftarrow}(X)$ in the unfolded state of the molecule. Note a distinct feature of the extension clamp setup: the observable (force) and the control parameter (extension) are switched with respect to those in the conventional manipulation modes.

In analogy with the instantaneous feedback idealization of the force clamp experiments, we will assume that the feedback of the extension clamp is sufficiently fast to consider the point X, which marks the total extension of the system, strictly stationary. Then the force exerted by the molecule-linker construct at this point at any moment of time is balanced by - and measured through - the instantaneous force $F(t)$ of the pulling spring, thus reporting the variations in $x(t)$. Assuming that $x(t)$ is a good reaction coordinate [15], the conformational dynamics of the system can be viewed as diffusive dynamics of $x(t)$ on the combined free energy profile

$$G(x|X) = G_0(x) + G_{pull}(X-x) \qquad \forall X = const. \quad (1)$$

Here $G_0(x)$ is the intrinsic free energy profile of the molecule and $G_{pull}(X-x)$ is the bias imposed on the intrinsic profile by the extension clamp via the linker whose extension at time t is $X - x(t)$ with $X = const$ (Fig.1B).

The expression in Eq.(1) can be recognized as the energy of an equivalent system of two (in general, anharmonic) springs connected in series at the point $x(t)$ with their total extension $x(t) + (X - x(t)) = X$ being fixed. For a harmonic linker, $G_{pull}(X-x) = \kappa(X-x(t))^2/2$; however, the harmonic approximation is generally not applicable to unstructured biopolymers, which results in a more complex form of the non-linearity of $G_{pull}(X-x)$. The dynamics on the combined potential $G(x|X)$ ultimately determines the lifetimes of the conformational states of the molecule, measured in experiment. However, experimental studies typically face the inverse problem: how to reconstruct the molecular energy landscape $G_0(x)$ given the observed lifetimes [16]. This task can be accomplished through establishing an analytical relationship between the lifetimes observed under perturbation and parameters of the landscape in the absence of perturbation. The goal of this work is to establish such a relationship. The parameters to be extracted from the analysis are indicated in Fig.1B: the intrinsic lifetimes of the folded ($\tau^0_{\rightarrow}$) and unfolded ($\tau^0_{\leftarrow}$) states, and the locations ($\Delta x^{\ddagger}_{\rightarrow}$ and $\Delta x^{\ddagger}_{\leftarrow}$) and heights ($\Delta G^{\ddagger}_{\rightarrow}$and $\Delta G^{\ddagger}_{\leftarrow}$) of the free energy barriers to unfolding and to refolding.

Just as any physical constraint imposed on a molecule, an extension clamp perturbs the molecular energy landscape. However, this perturbation is (i) non-linear in x (Fig.1B), in contrast to the linear bias, $-Fx$, in a force clamp at a force F, and (ii) static with respect to a given molecular configuration x, in contrast to the time-dependent bias, $\kappa_s\left(vt - X(t)\right)^2/2$, in the constant speed experiment at a speed v and a spring constant κ_s.

Figure 2 illustrates how the distinct way in which the extension clamp alters the molecular landscape endows this manipulation mode with unique capabilities. Generally, optimal conditions for the exchange ("hopping") between the folded and unfolded states are realized at the force $F_{1/2}$ in the force clamp and at the extension $X_{1/2}$ in the extension clamp, when the potential is tilted to the extent where unfolding and refolding transitions are equally probable. However, observations of "hopping" in a force clamp have been limited to systems with small energy barriers [17–19] because the barrier separating two conformations at $F_{1/2}$ is usually too high for "hopping" to occur in abundance on the experimental time scale. Remarkably, the extension clamp overcomes this difficulty by the very nature of the bias it imposes on the molecular potential: due to the non-linearity of this bias, the barrier separating the two conformations at $X_{1/2}$ in the extension clamp is lower than the same barrier at $F_{1/2}$ in the force clamp (Fig.2, vertical double arrows).

The non-linearity of the extension clamp bias has exploitable consequences. First, due to the lifetime at $X_{1/2}$ being shorter than the lifetime at $F_{1/2}$ for the same transition (Fig.4), an extension clamp produces kinetic records rich with "hopping" within the experimental timescale. Second, in systems with multiple barriers,

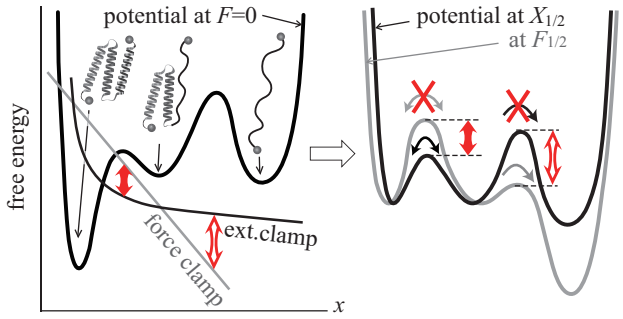

FIG. 2: Left: Potential at zero force. Right: Shown in grey is the potential at force $F_{1/2}$ for the leftmost barrier. Shown in black is the potential at extension $X_{1/2}$ for the same barrier. The nonlinear bias imposed by the extension clamp makes the leftmost barrier at $X_{1/2}$ lower and, consequently, the corresponding reversible transition more frequent than at $F_{1/2}$. On a potential with multiple minima, the non-linear bias in the extension clamp is likely to favor a persistent reversible transition whereas the force clamp and the force ramp favor sequential irreversible transitions.

the extension clamp can make persistent back-and-forth transitions over a particular barrier, whereas the force clamp/ramp favor a unidirectional escape along the sequential barriers such that the reversible transitions are observed, at best, transiently. Indeed, when a helical membrane protein (Fig.2) is held in a force clamp or a force ramp, the helices tend to unfold sequentially and irreversibly [20] because the barrier to further unfolding is lower than the barrier to refolding. In contrast, an extension clamp may allow for a single helix to undergo persistent unfolding-refolding in and out of the membrane while the rest of the protein remains intact, because the barrier to further unfolding is now higher than the barrier to refolding. Note that, despite the non-linear bias in the force ramp, the pulling spring is continuously retracted, making "hopping" likely only at very slow pulling [21].

Expressions for the extension-dependent lifetimes for unfolding ($\rightarrow$) and refolding ($\leftarrow$) transitions can be derived from Kramers theory [22] adapted to the diffusion on a potential perturbed by the extension clamp:

$$\tau_{\rightleftharpoons}(X) = D^{-1}\int_{\cup} dx e^{-\beta G_{\rightleftharpoons}(x|X)}\int_{\cap} dx e^{\beta G_{\rightleftharpoons}(x|X)}. \quad (2)$$

Here, the integrals span the regions of the folded/unfolded well ($\cup$) and the barrier ($\cap$) on the combined potential $G(x|X)$ in Eq.(1), D is the effective diffusion coefficient, and $\beta = 1/k_BT$. To perform the integration, we need to specify the functional form of $G_0(x)$ and $G_{pull}(X-x)$ in Eq.(1).

To design $G_0(x)$, we note that an exchange between two conformations can be modeled by the dynamics on a double-well potential. While the narrow folded state behaves as a harmonic well, the broad unfolded state is usually anharmonic which makes its behavior under force strikingly different [23] from that of its harmonic idealization. We find that the following form of the intrinsic potential of the molecule not only captures the worm-like chain nature of the unfolded state but also keeps the problem analytically tractable: $G_0^{\rightleftharpoons}(x) = \Delta G^{\ddagger}_{\rightarrow} - \frac{1}{\nu_{\rightleftharpoons}}\frac{\Delta G^{\ddagger}_{\rightleftharpoons}}{\Delta x_{\rightleftharpoons}}\left|x-\Delta x^{\ddagger}_{\rightarrow}\right| + \frac{1-\nu_{\rightleftharpoons}}{\nu_{\rightleftharpoons}}\frac{\Delta G^{\ddagger}_{\rightleftharpoons}}{\Delta x_{\rightleftharpoons}^{\ddagger 1/(1-\nu_{\rightleftharpoons})}}\left|x-\Delta x^{\ddagger}_{\rightarrow}\right|^{1/(1-\nu_{\rightleftharpoons})}$, where $\nu_{\rightleftharpoons}$ tune the degree of anharmonicity of the folded ($\nu_{\rightarrow}$) and unfolded ($\nu_{\leftarrow}$) wells, with $\nu_{\rightleftharpoons} = 1/2$ for a harmonic well (Fig.3A).

To specify $G_{pull}(X-x)$, we exploit a relationship between the potentials of a molecule in the extension clamp at X and in the force clamp at $F = F_{\rightleftharpoons}(X)$ (Fig.3B): $G^{\rightleftharpoons}_{\text{ext. clamp}}(x|X) \approx \phi_{\rightleftharpoons}(X)G^{\rightleftharpoons}_{\text{force clamp}}(x|F_{\rightleftharpoons}(X))$ [23]. Here $\phi_{\rightarrow}$ ($\phi_{\leftarrow}$) is the ratio of the barrier heights for unfolding (refolding) in the two types of experiment: $\phi_{\rightleftharpoons}(X) \equiv \frac{\Delta G^{\rightleftharpoons}_{\text{ext. clamp}}(X)}{\Delta G^{\rightleftharpoons}_{\text{force clamp}}(F_{\rightleftharpoons}(X))}$. Re-writing the integrands in Eq.(2) as $e^{-\beta\phi_{\rightleftharpoons}(X)\left[G_0^{\rightleftharpoons}(X)-F_{\rightleftharpoons}(X)x\right]}\ldots$ and omitting $\phi_{\rightleftharpoons}(X)$ in the pre-exponential factor, we obtain the closed-form solutions for the lifetimes in the extension clamp, where the upper (lower) subscript in the $\rightleftharpoons$ notations corresponds to the unfolding (refolding) process:

$$\tau_{\rightleftharpoons}(X) = \tau^0_{\rightleftharpoons}\frac{\left(1\mp\nu_{\rightleftharpoons}\Delta x^{\ddagger}_{\rightleftharpoons}F_{\rightleftharpoons}(X)/\Delta G^{\ddagger}_{\rightleftharpoons}\right)^{\frac{1}{2\nu_{\rightleftharpoons}}-2}}{\left(1\pm\nu_{\leftrightarrows}\Delta x^{\ddagger}_{\leftrightarrows}F_{\leftrightarrows}(X)/\Delta G^{\ddagger}_{\leftrightarrows}\right)}$$
$$\times\exp\left\{\beta\Delta G^{\ddagger}_{\rightleftharpoons}\left[\phi_{\rightleftharpoons}(X)\left(1\mp\frac{\nu_{\rightleftharpoons}\Delta x^{\ddagger}_{\rightleftharpoons}F_{\rightleftharpoons}(X)}{\Delta G^{\ddagger}_{\rightleftharpoons}}\right)^{\frac{1}{\nu_{\rightleftharpoons}}}-1\right]\right\} \quad (3)$$

with the forces $F_{\rightleftharpoons}(X)$ observed in the force trajectories (Fig.3B). Note that $\tau_{\rightarrow}(X)$ for escape from the folded state depends on the parameters of the unfolded state, and vice versa, as a consequence of the unfolding and refolding processes sharing the same barrier.

To determine $\phi_{\rightleftharpoons}(X)$ in Eq.(3), we express the "stiffness" of the folded and unfolded states of the molecule-linker system as the derivative of the force in the corresponding state with respect to the total extension: $\kappa_{\rightleftharpoons}(X) = \partial F_{\rightleftharpoons}(X)/\partial X$. The forces $F_{\rightleftharpoons}(X)$, in turn, can be written as the derivatives of the "pulling" potential $G^{\rightleftharpoons}_{pull}(X-x)$ [23]. Solving for the inverse of $\phi_{\rightleftharpoons}(X)$ gives

$$\phi^{-1}_{\rightleftharpoons}(X) = 1-\frac{(1-\nu_{\rightleftharpoons})\Delta x^{\ddagger\,2}_{\rightleftharpoons}\kappa_{\rightleftharpoons}(X)}{\Delta G^{\ddagger}_{\rightleftharpoons}}\left(1\mp\frac{\nu_{\rightleftharpoons}\Delta x^{\ddagger}_{\rightleftharpoons}F_{\rightleftharpoons}(X)}{\Delta G^{\ddagger}_{\rightleftharpoons}}\right)^{\frac{1}{\nu_{\rightleftharpoons}}-2} \quad (4)$$

In practice, the values of $\kappa_{\rightarrow}(X)$ and $\kappa_{\leftarrow}(X)$, entering Eq.(4), can be extracted directly from the slopes of the force-extension graphs at the corresponding X for unfolding and refolding events, respectively (Fig.3B).

The analytical form of Eq.(3) makes it readily suitable for a least-squares fit of the lifetimes measured in an extension clamp experiment. Fitting produces the parameters (indicated in Fig.1B and Fig.3A) of the intrinsic free energy landscape of the molecule. Furthermore, the activation barriers, extracted from a fit to the theory, yield the equilibrium free energy, $\Delta G = \Delta G^{\ddagger}_{\leftarrow} - \Delta G^{\ddagger}_{\rightarrow}$.

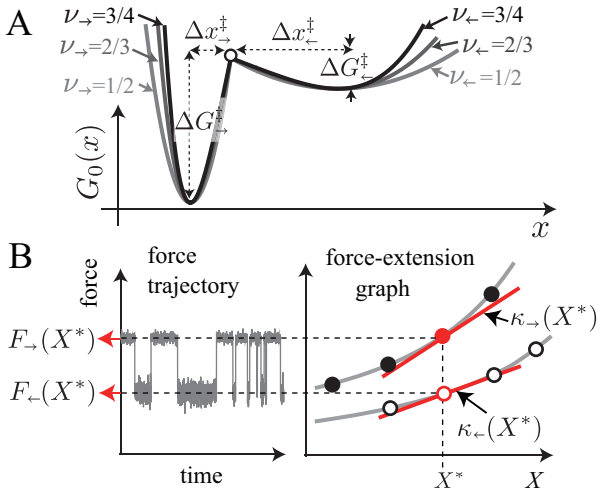

FIG. 3: (a) The intrinsic potential $G_0(x)$ captures the anharmonic nature of the unfolded state through the value of $\nu_{\leftarrow}$, with $\nu_{\leftarrow} = 1/2$ corresponding to a harmonic well. (b) *Left*: Force vs. time trajectory from the Brownian dynamics simulation on a system with the intrinsic potential shown in (a) held at a fixed extension $X = X^*$. The force "hops" between $F_{\rightarrow}(X^*)$ in the folded state and $F_{\leftarrow}(X^*)$ in the unfolded state. *Right*: Force-extension graph from which $\kappa_{\rightleftarrows}(X)$ in Eq.(4) can be extracted as the slope of the unfolding/refolding force at the corresponding value of X.

The analytical theory in Eqs.(3,4) was tested against numerical mean-first-passage-time [24] data from potentials that capture the worm-like chain behavior [25] of the linker and the unfolded state of the molecule (details in [23]). In the light of potential applications of the present framework, we considered three sets of parameters representative of (i) a medium-size globular protein [21, 26], (ii) a protein alpha-helix [20] (Fig.4) and (iii) a fragment of an alpha-helix. A unique parameter set $\{\tau^0_{\rightleftarrows}, \Delta G^{\ddagger}_{\rightleftarrows}, \Delta x^{\ddagger}_{\rightleftarrows}, \nu_{\leftarrow}\}$ for each system was determined by fitting the unfolding and refolding data *simultaneously*, with $\nu_{\rightarrow}$ fixed at 1/2, reflective of a harmonic folded state. To account for a limited time resolution and instrumental drift in experiment, we excluded the potentially inaccessible values of X from the fit (Fig.4, grey symbols). The agreement between theory and data both inside and, remarkably, outside the range used in the fit, along with the accurately recovered parameter values (Fig.4, Table 1 and [23]) confirm the validity of the theory.

How are the force- and extension-dependent lifetimes, measured in different types of experiments on the same system, related? To establish the mapping, we first compute the lifetimes at constant force F [16] from Kramers expression, Eq.(2), now applied to the combined potential $G(x|F) = G_0(x) - Fx$ with $G_0(x)$ introduced above:

$$\tau_{\rightleftarrows}(F) = \tau^0_{\rightleftarrows} \frac{\left(1 \mp \nu_{\rightleftarrows}\Delta x^{\ddagger}_{\rightleftarrows} F/\Delta G^{\ddagger}_{\rightleftarrows}\right)^{\frac{1}{2\nu_{\rightleftarrows}}-2}}{\left(1 \pm \nu_{\leftrightarrows}\Delta x^{\ddagger}_{\leftrightarrows} F/\Delta G^{\ddagger}_{\leftrightarrows}\right)}$$

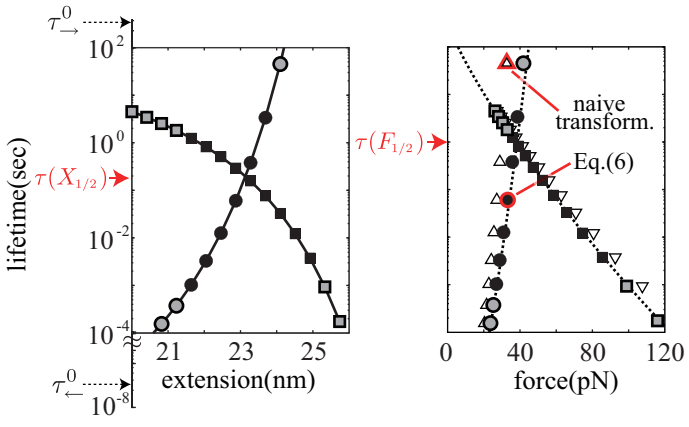

FIG. 4: *Left*: Lifetimes from the extension clamp: simulated data (symbols) and fit to theory, Eq.(3) (solid lines). Note that the data excluded from the fit (grey symbols) to mimic experimental limitations are accurately reproduced by the theory. *Right*: Lifetimes from the extension clamp, shown on the left, transformed using mapping equation, Eq.(6), agree with force clamp simulated data (dotted lines). Naïve transformation $\tau_{\rightleftarrows}(X) \approx \tau_{\rightleftarrows}(F = F_{\rightleftarrows}(X))$ (triangles) leads to significant errors (compare the two data points in red).

$$\times \exp\left\{\beta\Delta G^{\ddagger}_{\rightleftarrows}\left[\left(1 \mp \frac{\nu_{\rightleftarrows}\Delta x^{\ddagger}_{\rightleftarrows} F}{\Delta G^{\ddagger}_{\rightleftarrows}}\right)^{1/\nu_{\rightleftarrows}} - 1\right]\right\}. \quad (5)$$

It is worth noting that Eq.(5) naturally relates the value of $\nu_{\leftarrow}$ to the degree of anharmonicity of the unfolded state (Fig.3A), particularly relevant for the lifetime $\tau_{\leftarrow}(F)$ for the refolding process. Comparing the exponential factors, dominating the kinetics, in Eq.(3) and Eq.(5), we arrive at the following mapping between data in the two types of experiments:

$$\tau_{\rightleftarrows}(X) \approx \tau_{\rightleftarrows}\left(F = F_{\rightleftarrows}(X)\phi^{\nu_{\rightleftarrows}}_{\rightleftarrows}(X) \pm \frac{\Delta G^{\ddagger}_{\rightleftarrows}}{\nu_{\rightleftarrows}\Delta x^{\ddagger}_{\rightleftarrows}}\left[1 - \phi^{\nu_{\rightleftarrows}}_{\rightleftarrows}(X)\right]\right) \quad (6)$$

This transformation converts a lifetime data point from an extension clamp experiment into the lifetime that would be measured in a force clamp experiment at the force indicated as the argument on the right hand side of Eq.(6). In particular, Eq.(6) grants access to the kinetics around $F_{1/2}$ when large activation barriers make this force range inaccessible in the force clamp. Mapping in Eq.(6) is successfully realized in Fig.4 (right). The validity of the transformation was further confirmed at the parameters representative of other systems [23]. Figure 4 also highlights the inaccuracy of the naïve conversion $\tau_{\rightleftarrows}(X) \approx \tau_{\rightleftarrows}(F = F_{\rightleftarrows}(X))$ (triangles).

In summary, the theoretical framework developed here provides kinetic and energetic parameters of a macromolecule manipulated in an extension clamp. The derived analytical solutions for the key experimental outputs are rich in mechanistic information. An extension clamp is shown to possess the inherent capacity to measure the exchange between conformational states that would otherwise only occur scarcely or transiently.

TABLE I: Intrinsic parameters of the free energy landscape extracted from the fit (Fig.4) of the numerical mean-first-passage-time extension-clamp data to analytical solutions in Eqs.(3) and (4).

	$\tau^0_{\rightarrow}$ (sec)	$\tau^0_{\leftarrow}$ (sec)	$\Delta G^{\ddagger}_{\rightarrow}(k_BT)$	$\Delta G^{\ddagger}_{\leftarrow}(k_BT)$	$\Delta x^{\ddagger}_{\rightarrow}$ (nm)	$\Delta x^{\ddagger}_{\leftarrow}$ (nm)	$\nu_{\leftarrow}$
actual	2.89×10^2	2.67×10^{-8}	27.0	2.0	0.50	1.00	-
fit	2.72×10^2	2.17×10^{-8}	28.1	1.8	0.55	0.98	0.520

We are grateful to Robert Best, Steven Block, Gavin King, Florian Kämpfer, Hongbin Li, Tom Perkins, Christopher Pierse and Yaojun Zhang for valuable discussions. This research was supported by NSF CAREER Grant MCB-0845099 and NSF CTBP Grant PHY-0822283.

[1] N. de Souza, Nature Methods **9**, 873 (2012).
[2] K. Visscher, M. J. Schnitzer, and S. M. Block, Nature **400**, 184 (1999).
[3] A. Oberhauser, P. Hansma, M. Carrion-Vazquez, and J. Fernandez, Proc. Natl. Acad. Sci. U.S.A. **98**, 468 (2001).
[4] W. J. Greenleaf, M. T. Woodside, E. A. Abbondanzieri, and S. M. Block, Phys. Rev. Lett. **95**, 208102 (2005).
[5] M. Rief, M. Gautel, F. Oesterhelt, J. Fernandez, and H. Gaub, Science **276**, 1109 (1997).
[6] E. Evans, and K. Ritchie, Biophys. J. **72**, 1541 (1997).
[7] A. Gordon, A. Huxley, and F. Julian, J. Physiol. **184**, 143 (1966).
[8] R. Simmons, J. Finer, S. Chu, and J. Spudich, Biophys. J. **70**, 1813 (1996).
[9] M. Wang, H. Yin, R. Landick, J. Gelles, and S. Block, Biophys. J. **72**, 1335 (1997).
[10] K. Visscher, and S. Block, Methods Enzymol. **298**, 460 (1998).
[11] D. Keller, D. Swigon, and C. Bustamante, Biophys. J. **84**, 733 (2003).
[12] U. Gerland, R. Bundschuh, and T. Hwa, Biophys. J. **84**, 2831 (2003).
[13] G. M. King, A. R. Carter, A. B. Churnside, L. S. Eberle, and T. T. Perkins, Nano Letters **9**, 1451 (2009).
[14] G. M. King, A. B. Churnside, and T. T. Perkins, Biophys. J. **98**, 588a (2010).
[15] O. K. Dudko, T. G. W. Graham, and R. B. Best, Phys. Rev. Lett. **107**, 208301 (2011).
[16] O. K.Dudko, and G. Hummer, and A. Szabo, Phys. Rev. Lett. **96**, 108101 (2006).
[17] J. Liphardt, B. Onoa, S. B. Smith, I. Tinoco, and C. Bustamante, Science **292**, 733 (2001).
[18] M. T. Woodside, P. C. Anthony, W. M. Behnke-Parks, K. Larizadeh, D. Herschlag, and S. M. Block, Science **314**, 1001 (2006).
[19] C. Cecconi, E. A. Shank, C. Bustamante, and S. Marqusee, Science **309**, 2057 (2005).
[20] F. Oesterhelt, D. Oesterhelt, M. Pfeiffer, A. Engel, and H. Gaub, D. J. Muller, Science **288**, 143 (2000).
[21] J. P. Junker, F. Ziegler, and M. Rief, Science **323**, 633 (2009).
[22] H. Kramers, Physica **7**, 284 (1940).
[23] See Supplemental Material at ... for details of the derivations; generating numerical data; validation of the theory at the parameter sets representative of other systems.
[24] R. Zwanzig, *Nonequilibrium Statistical Mechanics* (Oxford University Press, Inc., 2001).
[25] J. Marko, and E. Siggia, Macromolecules **28**, 8759 (1995).
[26] T. Shen, Y. Cao, S. Zhuang, and H. Li, Biophys. J. **103**, 807 (2012).